

# Degradation of Nonylphenol Ethoxylate-9 (NPE-9) by Photochemical Advanced Oxidation Technologies

Luciana de la Fuente,<sup>†</sup> Tatiana Acosta,<sup>†,‡</sup> Paola Babay,<sup>†</sup> Gustavo Curutchet,<sup>‡,§,||</sup> Roberto Candal,<sup>‡,§,||</sup> and Marta I. Litter<sup>\*,†,§,||</sup>

Gerencia Química, Comisión Nacional de Energía Atómica, Avenida General Paz 1499, 1650 San Martín, Provincia de Buenos Aires, Argentina, Escuela de Ciencia y Tecnología, Universidad de General San Martín, 25 de Mayo y Martín de Irigoyen, 1650 San Martín, Provincia de Buenos Aires, Argentina, Instituto de Investigación e Ingeniería Ambiental, Universidad de General San Martín, Peatonal Belgrano 3563, 1650 San Martín, Provincia de Buenos Aires, Argentina, and Consejo Nacional de Investigaciones Científicas y Técnicas, Buenos Aires, Argentina

The applicability of different photochemical advanced oxidation technologies (PAOTs), namely, direct UV-C photolysis, UV-C/H<sub>2</sub>O<sub>2</sub> and UV-A/TiO<sub>2</sub> heterogeneous photocatalysis (HP), and photo-Fenton reactions (UV-A/H<sub>2</sub>O<sub>2</sub>/Fe<sup>2+</sup>, PF), for the degradation of 300 mg L<sup>-1</sup> nonylphenol ethoxylate-9 (NPE-9) in water is described. Different kinetic regimes for each PAOT were found, and as a result, comparative efficiencies could be obtained only from final parameters such as NPE-9 conversion, TOC decrease, and aldehyde production after 3 h of treatment. The initial photonic efficiencies indicate, however, that UV-A processes make better use of photons than UV-C processes. Preliminary optimization of PF systems showed that the most efficient NPE-9/H<sub>2</sub>O<sub>2</sub>/Fe<sup>2+</sup> molar ratio was 1:1:0.5. Degradation products were partially investigated. Fortunately, toxic 4-nonylphenol was never found as a byproduct of the degradation after any of the treatments. Aldehydes were formed in all of the processes, but they appeared at a low extent in PF reactions. Therefore, PF treatments were considered to be the best degradation processes.

## Introduction

Alkylphenol ethoxylates (alkylphenoxyethers, APEs) are a group of nonionic surfactants that are most often used in detergents, emulsifiers, and dispersing agents in household, agricultural, and industrial applications.<sup>1–3</sup> However, although the toxicity of APEs is relatively low, concern over their widespread use has increased in recent times because their biodegradation is slow and they generate highly toxic stable and biorefractory metabolites, especially those with one or two ethoxylate groups or those with none (alkylphenols).<sup>3–9</sup> These substances are considered endocrine-disrupting chemicals, that is, substances that alter the normal functioning of the hormonal system of mammals, fishes, and amphibians.<sup>1,3,9–16</sup> In addition, the presence of APEs in biological treatment plants causes serious problems because of their ability to produce foams, decreasing the capacity for oxygen transfer and disturbing the processes of primary sedimentation, thus rendering biodegradation inefficient and incomplete.

For this reason, biological treatment of APEs has been questioned, and considering that these compounds continue to be used in many applications, procedures for degradation have to be improved. Techniques such as solvent extraction, activated-carbon adsorption, ion exchange, electrochemical treatments, incineration, or conventional oxidation can be very expensive, yield unwanted solid residues, require large amounts of chemicals or energy, or be ineffective for low pollutant concentrations.

Among APEs, nonylphenol ethoxylates [*p*-nonylphenyl poly(oxyethylene) ethers, denoted NPE-*n*, where *n* is the number of ethoxy groups linked to the aromatic ring] are widely used, with NPE-9 (Figure 1) being one of the most common nonionic surfactants.<sup>9</sup> This compound is in the limit of biodegradability (75%),<sup>17</sup> according to the Argentine IRAM regulation, which defines that a substance is biodegradable if it can be 80% degraded after 28 days of biological treatment.<sup>18</sup>

Photochemical advanced oxidation technologies (PAOTs) are innovative technologies for water decontamination that allow total or partial elimination of compounds resistant to conventional treatments. Among them, direct UV-C photolysis, UV-C/H<sub>2</sub>O<sub>2</sub>, photo-Fenton (PF), and TiO<sub>2</sub> heterogeneous photocatalysis (HP) are the most investigated.<sup>19–21</sup> In the literature, there are various examples of the treatment of APEs by PAOTs, a number of them using TiO<sub>2</sub> photocatalysis.<sup>6,9,10,17,22–31</sup> Degradation of NPE-9 by sonolysis has also been reported,<sup>3,15</sup> but this method seems to be little operative above the critical micellar concentration (CMC).<sup>3</sup> Electrochemical oxidation at modified SnO<sub>2</sub> electrodes has also been tested.<sup>16</sup> Ozonation was proposed, but it yielded low total organic carbon (TOC) removal and the main generated products were hazardous alkylphenols.<sup>5,32–34</sup> Fe(III)-photoinduced processes<sup>1</sup> and Fenton's reagent [1:1 Fe(II)/H<sub>2</sub>O<sub>2</sub> molar ratio] gave good results, and the latter was proposed as a pretreatment for a biological treatment.<sup>35</sup> Degradation of NPE-*n* by both UV-B and UV-A irradiation has been described.<sup>4,10</sup> However, UV-C treatments, with or without hydrogen peroxide, have not been described in the literature as methods to treat APEs. More importantly, most of the references were published a decade ago; there are no

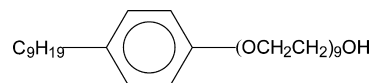


Figure 1. Structural formula of nonylphenol ethoxylate-9 (NPE-9).

\* To whom correspondence should be addressed. Tel.: +54-11-6772-7016. Fax: +54-11-6772-7886. E-mail: litter@cnea.gov.ar.

<sup>†</sup> Comisión Nacional de Energía Atómica.

<sup>‡</sup> Escuela de Ciencia y Tecnología, Universidad de General San Martín.

<sup>§</sup> Instituto de Investigación e Ingeniería Ambiental, Universidad de General San Martín.

<sup>||</sup> Consejo Nacional de Investigaciones Científicas y Técnicas.

comparisons among different techniques; and new details of the work merit study, especially at concentrations higher than the CMC. The final goal of such an effort is to apply a PAOT to increase biodegradability for further combination with a biological treatment to reduce total costs; this will be treated in a subsequent publication.

In this work, a comparison of some PAOTs, namely, UV-C, UV-A/HP, and UV-A/PF, for NPE-9 degradation is reported.

## Experimental Section

**Chemicals.** All chemicals were reagent grade and were used without further purification. TiO<sub>2</sub> (Degussa P-25) was provided by Degussa AG Germany and used as received. NPE-9 was obtained commercially as Tergitol (Sigma-Aldrich). According to the provider of Tergitol (Dow Chemical), the product is composed by poly(oxy-1,2-ethanediyl),  $\alpha$ -(4-nonylphenyl)- $\omega$ -hydroxy-, branched (>97%), polyethylene glycol (<3%), and dinonylphenyl polyoxyethylene (<2%).<sup>36</sup> 4-Nonylphenol (Fluka) and hydrogen peroxide (30%, Merck) were also used. Iron was added as ferrous perchlorate (Aldrich, analytical grade). For pH adjustments, dilute HClO<sub>4</sub> was used.

Water was purified (resistivity = 18 M $\Omega$ ·cm) with an E-pure Barnstead apparatus.

For high-performance liquid chromatography (HPLC) measurements, HPLC-grade sodium 1-octanesulfonate (Kodak), sodium acetate (Mallinckrodt), acetic acid (Cicarelli), and HPLC-grade acetonitrile (Merck) were used. For analytical determinations, ammonium acetate (Baker), acetylacetone (p.a., Merck), and 35–37% formaldehyde solution (Riedel-de Haën AG) were employed.

**Irradiation Procedures.** HP and PF experiments were performed in a batch recirculating system (1.0 L min<sup>-1</sup> flow rate) consisting of an annular glass reactor (415-mm length, 32-mm internal diameter), a peristaltic pump (APEMA BS6, 50 W), and a thermostatted (298 K) cylindrical reservoir. A black-light tubular UV lamp (Philips TLD/08, 15 W, 350 nm <  $\lambda$  < 410 nm, maximum emission at 366 nm) was installed inside the annular reactor as the illumination source. The total volume of the circulating mixture was 450 mL, of which 100 mL was inside the photoreactor and constantly irradiated.

For UV-C experiments, a similar annular photoreactor (420-mm length, 45-mm internal diameter) with a germicidal lamp (NIS, 15 W, G15T8, 254 nm) was used. In this case, the irradiated and total volumes were 350 and 700 mL, respectively. According to the UV spectrum of the lamp envelope, only wavelengths higher than 200 nm were emitted (i.e., emitting primarily at 254 nm, with no 185-nm irradiation entering the system).

The NPE-9 initial concentration in all experiments was 300 mg L<sup>-1</sup> (0.48 mM, considering an average molar mass of 616 g mol<sup>-1</sup> for NPE-9, although Tergitol is a mixture of several components; see later). This concentration is higher than the CMC (about 0.1 mM).<sup>37</sup> The initial pH of this solution is ca. 6. In experiments with H<sub>2</sub>O<sub>2</sub>, the corresponding volume of reagent was added immediately before starting the lamp. In UV-C/H<sub>2</sub>O<sub>2</sub> experiments, two initial NPE-9/H<sub>2</sub>O<sub>2</sub> molar ratios were tested, 1:1 and 1:0.5. In PF experiments, three initial NPE-9/H<sub>2</sub>O<sub>2</sub>/Fe<sup>2+</sup> molar ratios were chosen, namely, 1:1:0.1, 1:1:0.5, and 1:2:0.5; in these cases, the NPE-9 solution (450 mL) was first adjusted to pH 2.8 with dilute HClO<sub>4</sub>, and 1 mL of an adequate concentration of a fresh ferrous perchlorate solution (this Fe<sup>2+</sup> salt was chosen according to Pignatello<sup>47</sup>), to have the desired initial Fe(II) concentration, was added. Then, the corresponding H<sub>2</sub>O<sub>2</sub> volume was supplemented carefully before the lamp was

started. A similar experiment was performed in the dark with the 1:1:0.5 NPE-9/H<sub>2</sub>O<sub>2</sub>/Fe<sup>2+</sup> molar ratio (F). In HP experiments, TiO<sub>2</sub> was added at 1 g L<sup>-1</sup>, a concentration commonly used in our laboratory and in several other photocatalytic systems. The TiO<sub>2</sub> suspension was added to the NPE-9 solution, and the system was magnetically stirred for a few minutes and then ultrasonicated for 1 min. Then, suspensions were magnetically stirred for 30 min more in the dark to ensure the adsorption equilibrium of NPE-9 onto TiO<sub>2</sub>.

During irradiation, all solutions or suspensions were vigorously stirred in the reservoir. Air was bubbled throughout the experiments at a low flow to minimize foam formation (0.2 L min<sup>-1</sup>). Samples (5 mL) were periodically removed from the reservoir for analysis. HP samples were previously filtered through 0.2- $\mu$ m Sartorius cellulose acetate membranes. All experiments were performed at least in duplicate, and results were averaged. The experimental error was never higher than 12%.

Actinometric measurements were performed with ferrioxalate.<sup>38</sup> A photon flow per unit volume ( $q_p^0/V$ , where  $q_p^0$  is the incident photon flux and  $V$  is the irradiated volume) of 7.4  $\mu$ einstein s<sup>-1</sup> L<sup>-1</sup> was calculated for the black-light lamp (assuming 366-nm monochromatic light) and 7.0  $\times$  10<sup>-4</sup> einstein s<sup>-1</sup> L<sup>-1</sup> for the germicidal lamp (254-nm monochromatic light).

**Analysis of Samples.** Temporal NPE-9 concentration changes were followed by modification and combination of reported HPLC methods,<sup>39,40</sup> using an Alltech HPLC Pump model 301, a Spectra System UV1000 detector, and a Konikrom Chromatography Data System V.5.2. For detection, the signal at 277 nm (aromatic band) was registered. The following conditions were used: RP-C18 (Aquastar Hypurity, 5  $\mu$ m, 150  $\times$  4.6 mm column, pore size 190 Å); eluent, mixture of acetonitrile with a 4 mM sodium octanesulfonate and 0.02 M sodium acetate solution (pH 5.2 with acetic acid) in a 7:3 ratio. The flow rate was 1.0 mL min<sup>-1</sup>, and isocratic conditions at room temperature were employed. The injection loop was 100  $\mu$ L, and peak areas were adopted for measurements. The signal corresponding to NPE-9 appeared at a retention time ( $t_{ret}$ ) of 6 min. It was composed of a main central peak and poorly defined adjacent minor peaks (less than 3%), because the commercial product is a mixture of isomers and oligomers of different ethoxylated chains, from which the compound with nine ether units is the main one.<sup>7,10,36,41</sup> For the determination, only the area of the main peak was taken.

NPE-9 UV-vis spectra and their evolution with time were recorded with a diode-array Hewlett-Packard UV-visible spectrophotometer, model HP8453A.

TOC was measured with a Shimadzu 5000-A TOC analyzer in the nonpurgeable organic carbon (NPOC) mode. In what follows, we refer to this measurement simply as TOC.

Aldehyde formation was followed by the diacetylhydrotoluidine method,<sup>42</sup> monitoring the absorbance at 412 nm and using formaldehyde as the standard.

## Results and Discussion

**NPE-9 Decay in the Dark in the Presence of TiO<sub>2</sub>.** NPE-9 (300 mg L<sup>-1</sup>) adsorption on TiO<sub>2</sub> (1 g L<sup>-1</sup>) in the dark was tested before the photocatalytic experiments. The NPE-9 concentration decreased by around 14% after 10 min of stirring in the dark (data not shown), and these values held steady without variation for up to 240 min of stirring, indicating that no desorption phenomena took place in the time span of the

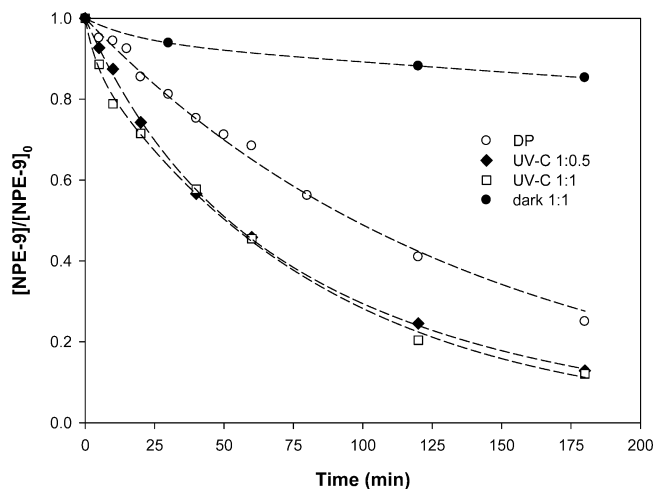


**Figure 2.** Time evolution of normalized NPE-9 concentration under UV-C irradiation. Conditions:  $[\text{NPE-9}]_0 = 300 \text{ mg L}^{-1}$  (0.48 mM),  $\text{pH}_0 \approx 6$ ,  $T = 298 \text{ K}$ ,  $q_p^0/V = 7.0 \times 10^{-4} \text{ einstein s}^{-1} \text{ L}^{-1}$ . The NPE-9/ $\text{H}_2\text{O}_2$  molar ratio is indicated. Dashed lines are double-exponential fits (see text).

experiments, at least in dark conditions. Therefore, HP runs were started after 30 min of stirring in the dark, to ensure enough time to reach adsorption equilibrium. After  $\text{TiO}_2$  addition, the pH decreased from 6 to around 5, indicating that NPE-9 adsorption releases protons to the solution.

**NPE-9 Decay in the PAOT Runs.** In the different PAOT runs, the temporal variation of the normalized NPE-9 concentration,  $[\text{NPE-9}]/[\text{NPE-9}]_0$ , where  $[\text{NPE-9}]_0$  is the initial concentration, was followed by HPLC.

The profiles for UV-C runs in the absence and in the presence of  $\text{H}_2\text{O}_2$  (1:1 and 1:0.5 NPE-9/ $\text{H}_2\text{O}_2$  molar ratios) are shown in Figure 2. Dark reactions with  $\text{H}_2\text{O}_2$  gave less than 15% degradation in 3 h, as shown for the 1:1 condition. It can be seen that, although NPE-9 could be very well degraded by UV-C light alone (reaching 75% depletion in 180 min),  $\text{H}_2\text{O}_2$  addition increased the rate, but no significant differences were found between the two  $\text{H}_2\text{O}_2$  concentrations used. As it is known,<sup>19–21</sup> cleavage of the  $\text{H}_2\text{O}_2$  molecule with photons of enough energy almost quantitatively produces two  $\text{HO}^\bullet$  radicals. Excess hydrogen peroxide can be detrimental because the reagent is a  $\text{HO}^\bullet$  scavenger. Therefore, the use of higher hydrogen peroxide concentrations was considered unnecessary and even inconvenient.

Temporal profiles of HP and PF runs, performed under UV-A irradiation, are shown in Figure 3. Almost total conversions were achieved in 180 min, showing a better efficiency than reactions under UV-C light (cf. Figures 2 and 3). The dark Fenton process was also effective, but with less transformation (around 60%). Intriguingly, HP runs presented a very rapid NPE-9 decay in the first 5 min of irradiation, then an arrest up to 40 min, followed by a further slightly slower degradation and a new arrest at 60 min. This indicates a very complex reaction system: intermediates probably block the  $\text{TiO}_2$  surface, impeding further NPE photocatalytic degradation until such blocking compounds are also degraded.<sup>43</sup>

Experimental data of Figures 2 and 3 (with the exception of the HP runs) could be fitted rather well by monoexponential curves; however, the fitting was even better ( $R^2 > 0.98$ ) using a double-exponential according to the expression

$$[\text{NPE-9}]/[\text{NPE-9}]_0 = a \exp(-k_1 t) + c \exp(-k_2 t) \quad (1)$$

and the constraint conditions  $k_1, k_2 > 0$ ,  $a + c = 1$ . This kinetics suggests the operation of two parallel mechanisms, one faster

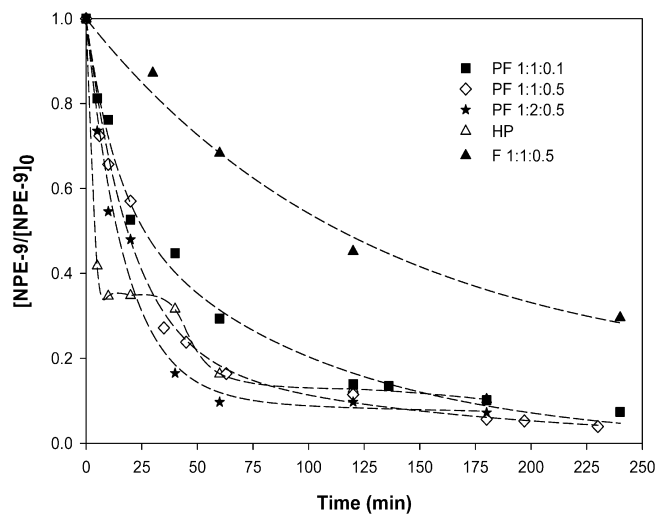


**Figure 3.** Time evolution of normalized NPE-9 concentration under different treatments using UV-A irradiation (HP and photo-Fenton). Conditions:  $[\text{NPE-9}] = 300 \text{ mg L}^{-1}$  (0.48 mM),  $\text{pH}_0 \approx 6$ ,  $T = 298 \text{ K}$ ,  $q_p^0/V = 7.4 \mu\text{einstein s}^{-1} \text{ L}^{-1}$ . The NPE-9/ $\text{H}_2\text{O}_2/\text{Fe}^{2+}$  molar ratio is indicated. In HP experiments,  $1 \text{ g L}^{-1} \text{ TiO}_2$  was used. A Fenton run is included. In the case of the PF and F systems, dashed lines are double-exponential fits (see text).

**Table 1. Kinetic Parameters for Double-Exponential Decays for the UV-C, Fenton, and Photo-Fenton Systems**

process	$a$	$k_1 \text{ (min}^{-1}\text{)}$	$b \text{ (min}^{-1}\text{)}$	$k_2 \text{ (min}^{-1}\text{)}$	$R^2$
dark NPE/ $\text{H}_2\text{O}_2$ (1:1)	0.06	0.052	0.94	0.001	1
UV-C (DP)*	0.49	0.007	0.51	0.007	0.994
UV-C/ $\text{H}_2\text{O}_2$ 1:0.5	0.26	0.033	0.74	0.010	1
UV-C/ $\text{H}_2\text{O}_2$ 1:1	0.10	0.257	0.90	0.011	0.998
F 1:1:0.5	0.85	0.008	0.15	$6 \times 10^{-15}$	0.989
PF 1:1:0.1	0.42	0.074	0.59	0.011	0.992
PF 1:1:0.5	0.78	0.050	0.22	0.007	0.986
PF 1:2:0.5	0.90	0.057	0.10	0.002	0.981

\* Same results for a simple exponential decay.

than the other, with the  $a$  and  $b$  parameters indicating the relative importance of each pathway; however, assignment to particular processes is very difficult. In contrast, no defined kinetic regime could describe the complex HP system.

Kinetic parameters are presented in Table 1. Reaction with  $\text{H}_2\text{O}_2$  in the dark almost follows a simple-exponential decay, and the only important process is the slowest one (represented by  $k_2$ ), because of the low value of  $a$ . The UV-C process without oxidants also follows a monoexponential regime. When  $\text{H}_2\text{O}_2$  is added (UV-C/ $\text{H}_2\text{O}_2$  systems), the fastest process, represented by  $k_1$ , is enhanced;  $k_2$  almost does not vary and remains the dominant process. Consequently, almost no kinetic differences could be observed between the two  $\text{H}_2\text{O}_2$  concentrations, as seen in Figure 2, indicating the small effect of a higher amount of  $\text{H}_2\text{O}_2$  on the overall kinetics under the present conditions. Turning now to the Fenton systems, in the case of the dark reaction (F), the slow process ( $k_2$ ) is nearly nonexistent. Under irradiation (PF), both  $k_1$  and  $k_2$  increase, but the effect of light on  $k_2$  is more significant. However, unlike in the UV-C cases, the process is dominated by the rapid pathway ( $k_1$ ). This rate constant is rather insensitive to the amount of both oxidants, Fe(II) and  $\text{H}_2\text{O}_2$ , whereas  $k_2$  reflects the deleterious effect of their excess. This analysis can be directly appreciated in Figure 3: Even though the dark process is the slowest one, light accelerates the reactions, and the addition of oxidants improves the processes in the first stages, being irrelevant at longer times.

**TOC Decrease.** Figure 4 shows the temporal evolution of TOC for all runs. The TOC reduction after 180 min of irradiation



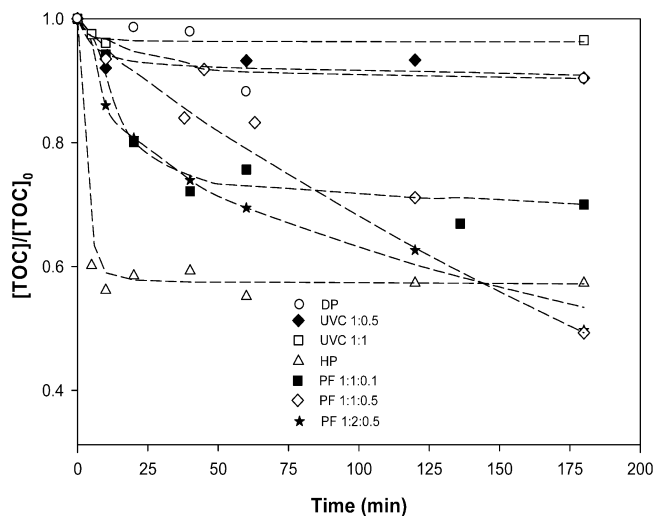


**Figure 4.** Time evolution of TOC in all PAOT processes. Conditions as in Figures 2 and 3.

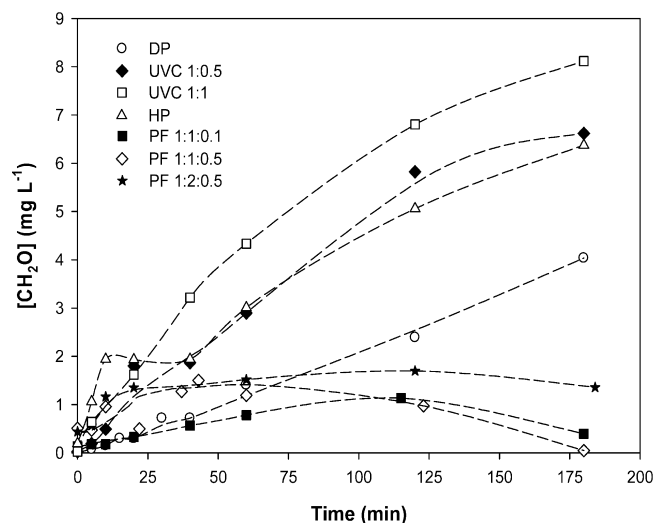


**Figure 5.** Time evolution of aldehydes produced in all PAOT processes. Conditions as in Figures 2 and 3.

was lower than the decrease of the NPE-9 concentration (compare Figures 2 and 3 with Figure 4). The TOC decrease was very low in the case of UV-C runs, attaining no more than ca. 10%, with all curves affected by significant experimental error because of the low TOC decrease. In the case of PF systems, an increase in  $\text{Fe}^{2+}$  concentration increased final TOC reduction, but in contrast, a higher  $\text{H}_2\text{O}_2$  amount did not lead to a further improvement. In the case of HP, TOC decreased rapidly in the first 5 min and then stopped, indicating the formation of recalcitrant intermediates.

**Aldehyde Formation.** The spectroscopic method used to follow the formation of aldehydes allows only for their quantification but not their identification. It is important to point out that air bubbling during the runs could have eliminated the most volatile homologues. Figure 5 shows the variation of the concentration of aldehydes during the different treatments, using formaldehyde as the standard. Considerable amounts of aldehydes were formed in HP and UV-C systems, especially in those containing  $\text{H}_2\text{O}_2$ , with more production at the highest  $\text{H}_2\text{O}_2$  concentration; their concentration never decreased in the time span of the experiments, paralleling the lack of TOC decrease. The same behavior was observed in previous studies of the  $\text{TiO}_2$  photocatalytic degradation of NPE-*n*.<sup>10</sup>

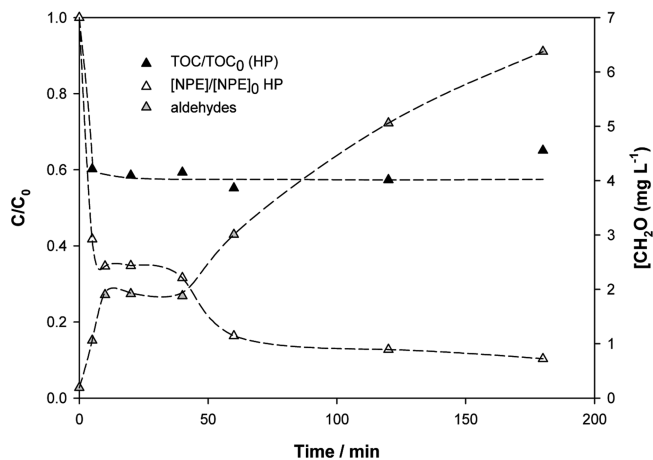


**Figure 6.** Correlation between NPE-9 decay, TOC decrease, and evolution of aldehydes during the HP runs. Conditions as in Figure 3.

In contrast, in PF systems, aldehydes were formed at low concentrations, reaching a maximum and then decreasing: this indicates further oxidation. Production of aldehydes was lower when low  $\text{H}_2\text{O}_2$  and high Fe concentrations were used (1:1:0.5 system), completely disappearing after 180 min.

The evolution of the three variables NPE-9 concentration, TOC decrease, and aldehyde formation in the HP run is shown in more detail in Figure 6: The TOC evolution matched the evolutions of NPE-9 and aldehydes during the first 40 min. As said before, the arrest of NPE-9 decay might be a consequence of the adsorption of intermediates on the  $\text{TiO}_2$  surface, which also hinders aldehyde production.<sup>43</sup> Later, when such blocking compounds begin to be degraded, the photocatalytic oxidation process starts again. However, intermediates seem to be very resistant to mineralization.

**Comparison of the Performance of Different Technologies.** All of the tested technologies gave rather good results for NPE-9 degradation at  $300 \text{ mg L}^{-1}$ , a concentration higher than the CMC. Direct 254-nm irradiation of a UV-photoactive molecule (direct photolysis, DP) leads to homolysis, heterolysis, or photoionization processes. Under irradiation, homolytic breakage produces radicals that initiate chain reactions, and in the presence of oxygen, reactive oxygen species (ROSs) such as superoxide ( $\text{O}_2^{\cdot-}$ ), hydroperoxyl ( $\text{HO}_2^{\cdot}$ ), and other radicals are generated, leading to transformation of the starting compound to aldehydes, ketones, or carboxylic acids.<sup>44</sup> Intermediate radicals and even impurities, typical in commercial compounds, can enhance oxidation. Although its efficiency is generally low, the UV-C process is rather economical because simple, low-cost, and easily available germicidal lamps (254 nm) can be used. In the present case, the low absorbance of NPE-9 at 254 nm ( $\epsilon = 283 \text{ M}^{-1} \text{ cm}^{-1}$ ; see later) explains the relatively low degradation in the absence of  $\text{H}_2\text{O}_2$ . The UV-C process can be improved by hydrogen peroxide addition.  $\text{H}_2\text{O}_2$  increases degradation, generating  $\text{HO}^{\cdot}$ , but the process is not as efficient as HP or PF probably because of the lower concentration of  $\text{HO}^{\cdot}$  and other ROSs generated, together with the simultaneous depletion of the oxidant.

The situation is different with HP and PF. According to the very well-known mechanisms,<sup>19,20,45–47</sup>  $\text{HO}^{\cdot}$  radicals are formed in these reactions at high concentrations, which is reflected by the higher observed initial rates (cf. Figures 2 and 3). In the dark Fenton process, the reaction stops gradually because  $\text{H}_2\text{O}_2$  (at the low concentration used in the present work) is consumed and  $\text{HO}^{\cdot}$  production is arrested. PF processes are very much

**Table 2. Initial Pseudo-First-Order Rate Constants ( $k_{in}$ ) and Initial Photonic Efficiencies ( $\xi_{in}$ ) Calculated at 5 min of Irradiation, Percentages of NPE-9 and TOC Abatement and Concentration of Aldehydes after a 3 h Process for All the Tested PAOTs<sup>a</sup>**

process	$k_{in}$ (min <sup>-1</sup> )	$\xi_{in}$ (%)	NPE-9 decay (%)	TOC decrease (%)	[CH <sub>2</sub> O] (mg L <sup>-1</sup> )
dark NPE/H <sub>2</sub> O <sub>2</sub> (1:1)	0.004	—	14.7	ND <sup>b</sup>	ND
UV-C (DP)	0.007	$8.46 \times 10^{-3}$	75.0	9.7	4.04
UV-C/H <sub>2</sub> O <sub>2</sub> 1:0.5	0.012	$1.47 \times 10^{-2}$	87.2	9.6	6.62
UV-C/H <sub>2</sub> O <sub>2</sub> 1:1	0.012	$1.59 \times 10^{-2}$	87.9	3.5	8.12
HP	0.175	18.9	89.7	42.7	6.37
F 1:1:0.5	0.006	—	~60	ND	ND
PF 1:1:0.1	0.042	4.50	92.6	30.0	0.39
PF 1:1:0.5	0.054	5.82	96.1	50.7	0.04
PF 1:2:0.5	0.067	7.78	92.8	50.3	1.36

<sup>a</sup> Data from Figures 2–5. <sup>b</sup> ND = not determined.

richer in reactive, strong oxidizing species, which are continuously produced.

Table 2 shows the initial rate constants ( $k_{in}$ , calculated from Figures 2 and 3 assuming pseudo-first-order kinetics up to 5 min of reaction) and the initial photonic efficiencies ( $\xi_{in}$ , calculated as the ratio of the initial rate of NPE-9 decay to the rate of incident photons of monochromatic light on the reactor window, eq 2). The data are in agreement with the above considerations. As can be seen, the  $k_{in}$  values are very similar to those indicated in Table 1 for the main processes in each case ( $k_1$  for F and PF and  $k_2$  for UV-C/H<sub>2</sub>O<sub>2</sub>).

$$\xi_{in} = \frac{(-dC/dt)_{t=0}}{q_p^0/V} \quad (2)$$

Photonic efficiencies of UV-C processes are very low, even though photon fluxes 2 orders of magnitude higher than those of UV-A processes were used. On the contrary,  $\xi_{in}$  for HP is very high, and the  $\xi_{in}$  values of the three PF processes are similar, although they increase with increasing amount of both oxidants.

On the other hand, the NPE-9 consumption, TOC decrease, and concentration of aldehydes at larger irradiation times (180 min) vary in a different way. Although NPE-9 decay is rather high after 3 h for all PAOTs, mineralization is lower, indicating, as already said, the formation of resistant intermediates. Both NPE-9 and TOC decay follow the same order, namely, HP  $\approx$  PF > UV-C; this indicates that UV-A processes are energetically more convenient, because a similar (or somewhat higher) conversion is reached with less waste of energy, making better use of photons. However, as the HP process loses its important high initial efficiency, PF systems are the best processes (high transformation of NPE-9 together with low production of aldehydes), with a better performance for the 1:1:0.5 ratio.

**pH Variation.** The original pH of NPE-9 solutions was around 6. At the beginning of HP runs, the pH decreased rather rapidly and then somewhat more slowly, arresting at pH ca. 4, in agreement with previous results.<sup>10</sup> Similar pH changes also took place during the UV-C treatments, with or without H<sub>2</sub>O<sub>2</sub>, although the pH decreased rather more slowly in the DP runs than in the other cases. These changes in pH suggest the formation of carboxylic acids. This variation could not be monitored in the photo-Fenton systems because the pH was kept constant at 2.8 throughout the reaction.

**Changes in the UV Spectra and in the Chromatograms during the Different Treatments.** The UV-vis spectrum of a 300 mg L<sup>-1</sup> NPE-9 solution at its original pH ( $\approx$ 6) is shown in Figure 7. Characteristic peaks, related to the aromatic structure of the molecule, appear around 200, 224, and 277 nm, in accordance with data reported for other alkylphenoxyethers.<sup>1,3,10</sup> As already said, NPE-9 absorption at 254 nm is low.

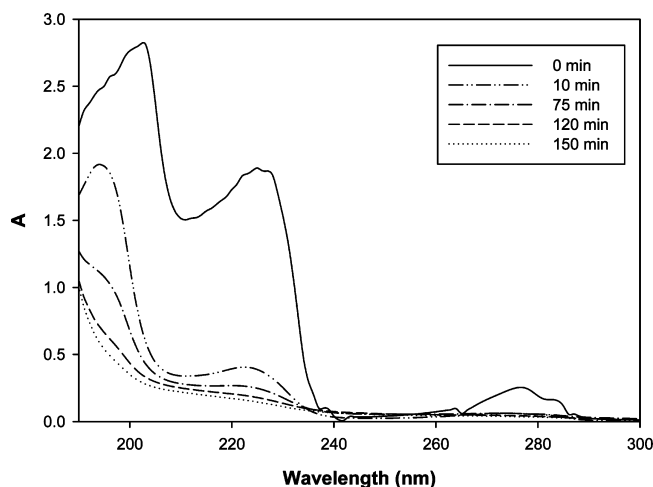


**Figure 7.** UV-vis spectral variation of NPE-9 (300 mg L<sup>-1</sup>) subjected to HP. Conditions as in Figure 3.

During HP experiments, the intensity of the peaks decreased rapidly as shown in the same Figure 7 (cf. peaks at 0 and 10 min), in agreement with the fast decrease observed by HPLC (see Figures 3 and 6), and no defined peaks could be seen after 120 min of irradiation, suggesting the opening of aromatic groups.

In the chromatograms of samples of all PAOT runs, a continuous decrease in the area of the characteristic NPE-9 peak was observed; in parallel, peaks of lower intensity were observed at a shorter retention time ( $t_{ret} \approx 2$  min), and their area increased constantly during the irradiation. The closeness with the dead time prevented us from making quantitative calculations from these peaks, but they certainly would correspond to degradation byproducts of lower molecular mass and/or higher acidity and polarity than NPE-9, in agreement with pH changes described in the preceding section; no efforts for their identification were made. The formation of these compounds would explain the remaining TOC even when NPE-9 could no longer be detected in solution.

Fortunately, comparison with a pure 4-nonylphenol standard confirmed that this toxic compound was not produced during the treatments at any stage. This agrees with previous results of TiO<sub>2</sub> photocatalysis of NPE-*n*<sup>17</sup> and contrasts with those obtained during the Fe(III)-photoinduced degradation of alkylphenol ethoxylates, where toxic alkylphenols were indeed identified as byproducts.<sup>1</sup>

**Preliminary Mechanistic Results.** Although this was not the purpose of the present work, the evidence of formation of aldehydes and carboxylic acids allows us to include preliminary comments on the mechanisms taking place during the PAOTs.

Concerning the reactive agents, in the case of the HP, PF, and UV-C/H<sub>2</sub>O<sub>2</sub> systems, HO<sup>•</sup> radicals are surely the main

species responsible for the degradation. In contrast, in the UV-C process in the absence of H<sub>2</sub>O<sub>2</sub>, no HO<sup>•</sup> is formed, and because the compound has a low absorption at 254 nm, the relatively significant degradation observed can be attributed only to the formation of active radicals in the presence of O<sub>2</sub> or impurities.

Previous detailed reports on the application of HP<sup>9,10,22–30</sup> or Fe(III)-photoinduced<sup>1</sup> processes on NPE-9 or similar compounds indicate the formation of different products. In these cases, HO<sup>•</sup> radical attack can take place at three different sites: the methylenic and methylic groups of the alkyl chain, the aromatic ring, and the methylenic groups of the ethoxylated moiety (see Figure 1). It has been proposed that the hydrogens in the ethoxylated part are more labile than those in the alkyl chain.<sup>13</sup> This differs from ultrasonic oxidation, where the alkyl chain has been found to be the preferential site.<sup>3</sup> On the other hand, radical attack on the aromatic ring has been proposed to be faster than hydrogen abstraction.<sup>10,17</sup> Therefore, after HO<sup>•</sup> addition to the aromatic group, the hydroxylated ring would open to evolve to CO<sub>2</sub> via several oxidation pathways, with the formation of aldehydes and carboxylic acids.

In the present case, examination of Figure 6 allows some conclusions can be drawn from the HP experiments. TOC decrease accompanies the fast NPE-9 decay in the first 10 min, suggesting attack on the aromatic moiety followed by decarboxylation, reinforced by changes in the spectrum of Figure 7 at 10 min. In parallel, HO<sup>•</sup> attack on the methylenic groups of the ethoxylated chains would also give rise to production of lower-molecular-mass intermediates, such as aldehydes, but without decarboxylation. Aldehyde production also parallels NPE-9 degradation in the first stages. As said before, there is a period of 30 min (from 10 to 40 min) where the intermediates would block the TiO<sub>2</sub> surface, with the arrest of NPE-9, TOC degradation, and aldehyde formation. After this period, these blocking compounds begin to be destroyed, with aldehyde formation and NPE-9 degradation starting again. However, the constancy of TOC at least until 180 min indicates the recalcitrance of the compounds to mineralization.

The UV-C/H<sub>2</sub>O<sub>2</sub> system has been never explored, and no details on possible intermediates existed previously; our results reveal the rather significant production of aldehydes, similarly to the HP case. In contrast, the negligible production of these compounds during PF processes suggests a different mechanism or the formation of more oxidizable species.

## Conclusions

HP, UV-C alone and with H<sub>2</sub>O<sub>2</sub>, and PF are convenient methods for treating NPE-9, although mineralization by UV-C processes is poor. Aldehydes and carboxylic acids are intermediate products of the reactions; fortunately, no toxic 4-nonylphenol is formed in any of the treatments. NPE-9 decay in UV-C, F, and PF runs could be fitted to double-exponential decays, indicating complex degradation; HP degradation follows an even more complicated mechanism according to the observed kinetic behavior.

Comparing the different assayed PAOTs, PF processes seem to be the optimal processes because of high NPE-9 and TOC decay, together with a reasonably high photonic efficiency, the poor formation of toxic aldehydes, and the lack of 4-nonylphenol formation. In a previous work,<sup>35</sup> the dark Fenton process was found to be useful for partially mineralizing NPE-*n*; however, high H<sub>2</sub>O<sub>2</sub> dosages were needed, and high concentrations of residual H<sub>2</sub>O<sub>2</sub> remained in the system, which is detrimental for effluent dumping or for the application of further biological treatment. In the PF systems explored here, a lower H<sub>2</sub>O<sub>2</sub> dose

is used, which implies an economic improvement, as chemicals have been found responsible for more than 90% of the total costs in similar systems.<sup>35</sup> It is possible to further optimize the PF system regarding the amount of reagents. On the contrary, although HP shows a very high initial photonic efficiency, the blocking of the TiO<sub>2</sub> surface leads to a serious arrest of the reaction; this, combined with the relatively high production of toxic aldehydes and the requirement for a further separation step for the powdered photocatalyst, makes this technique inconvenient. On the other hand, although their efficiencies are not very high, systems using UV-C with or without H<sub>2</sub>O<sub>2</sub> are simple and inexpensive, and their study merits continuation. Moreover, it is possible to take advantage of germicidal lamps used in common disinfection treatment plants.

Experiments for coupling PF systems with biological treatments are underway. It is important to remark that, for this purpose, all remaining H<sub>2</sub>O<sub>2</sub> should be eliminated and the pH should be increased to neutral values before the influent enters the biological reactor.

## Acknowledgment

This work was financed by the Comisión de Investigaciones Científicas de la Provincia de Buenos Aires (CICPBA), by the Universidad de General San Martín (SA08/011), and by the Agencia Nacional de la Promoción de la Ciencia y la Tecnología (ANPCyT, PAE 22257).

## Literature Cited

- (1) Brand, N.; Maillhot, G.; Bolte, M. Degradation photoinduced by Fe(III): Method of alkylphenol ethoxylates removal in water. *Environ. Sci. Technol.* **1998**, *32*, 2715.
- (2) Brand, N.; Maillhot, G.; Sarakha, M.; Bolte, M. Primary mechanism in the degradation of 4-octylphenol photoinduced by Fe(III) in water-acetonitrile solution. *J. Photochem. Photobiol. A: Chem.* **2000**, *135*, 221.
- (3) Destailhats, H.; Hung, H.-M.; Hoffmann, M. R. Degradation of alkylphenol ethoxylate surfactants in water with ultrasonic irradiation. *Environ. Sci. Technol.* **2000**, *34*, 311.
- (4) Chen, L.; Zhou, H.; Deng, Q. Photolysis of nonylphenol ethoxylates: The determination of the degradation kinetics and the intermediate products. *Chemosphere* **2007**, *68*, 354.
- (5) Hyunook, K.; Guisu, P.; Myongjin, Y.; Eunjung, K.; Youngkook, H.; Colosimo, M. K. Oxidation of Nonylphenol in Water Using O<sub>3</sub>. *Res. J. Chem. Environ.* **2007**, *11*, 72.
- (6) Ike, M.; Asano, M.; Belkada, F. D.; Tsunoi, S.; Tanaka, M.; Fujita, M. Degradation of biotransformation products of nonylphenol ethoxylates by ozonation and UV/TiO<sub>2</sub> treatment. *Water Sci. Technol.* **2002**, *46*, 127.
- (7) Lozada, M.; Itria, R.; Figuerola, E.; Babay, P.; Gettar, R.; de Tullio, L.; Erijman, L. Bacterial community shifts in nonylphenol polyethoxylates enriched activated sludge. *Water Res.* **2004**, *38*, 2077.
- (8) Ying, G.-G.; Williams, B.; Kookana, R. Environmental fate of alkylphenols and Alkylphenol ethoxylates—A review. *Environ. Int.* **2002**, *28*, 215.
- (9) Horikoshi, S.; Watanabe, N.; Onishi, H.; Hidaka, H.; Serpone, N. Photodecomposition of a nonylphenol polyethoxylate surfactant in a cylindrical photoreactor with TiO<sub>2</sub> immobilized fiberglass cloth. *Appl. Catal. B: Environ.* **2002**, *37*, 117.
- (10) Neamtu, M.; Frimmel, F. H. Photodegradation of endocrine disrupting chemical nonylphenol by simulated solar UV-irradiation. *Sci. Total Environ.* **2006**, *369*, 295.
- (11) Goto, R.; Kubota, T.; Ibuki, Y.; Kaji, K.; Goto, A. Degradation of nonylphenol polyethoxylates by ultraviolet B irradiation and effects of their products on mammalian cultured cells. *Toxicology* **2004**, *202*, 237.
- (12) European Parliament and Council. Decision no. 2455/2001/EG of 2001.11.10 on establishment of a list of compounds of priority in the area of water policy and on an amendment of directive 2000/60/EG (the EU frame directive of water).
- (13) Pelizzetti, E.; Minero, C.; Maurino, V.; Sclafani, A.; Hidaka, H.; Serpone, N. Photocatalytic degradation of nonylphenol ethoxylated surfactants. *Environ. Sci. Technol.* **1989**, *23*, 1380.
- (14) Hidaka, H.; Zhao, J. Photodegradation of surfactants catalyzed by a TiO<sub>2</sub> semiconductor. *Colloids Surf.* **1992**, *67*, 165.



- (15) Vinodgopal, K.; Ashokkumar, M.; Grieser, F. Sonochemical degradation of a polydisperse nonylphenol ethoxylate in aqueous solution. *J. Phys. Chem. B* **2001**, *105*, 3338.
- (16) Ihoş, M.; Manea, F.; Iovi, A. Removal of Nonylphenol Polyethoxylate by Electrochemical Oxidation at Modified SnO<sub>2</sub> Electrodes. *Chem. Bull. "POLITEHNICA" Univ. Timișoara* **2008**, *53*, 175.
- (17) Potarsky, K. Tratamiento de efluentes líquidos conteniendo nonilfenol por método biológico. Degree Thesis, Universidad de General San Martín, San Martín, Argentina, 2004.
- (18) Norma IRAM (Instituto Argentino de Normalización y Certificación) 25610, December 1994, "Agentes Tensioactivos: Determinación del grado de biodegradabilidad última".
- (19) Oppenländer, T. *Photochemical Purification of Water and Air—Advanced Oxidation Processes (AOPs): Principles, Reaction Mechanisms, Reactor Concepts*; Wiley-VCH: New York, 2003.
- (20) Litter, M. I. Introduction to photochemical advanced oxidation processes for water treatment. In *The Handbook of Environmental Chemistry*; Boule, P., Bahnemann, D. W., Robertson, P. K. J., Eds.; Springer-Verlag: Berlin, 2005; Vol. 2, Part M, pp 325–366.
- (21) Pera-Titus, M.; García-Molina, V.; Baños, M. A.; Giménez, J.; Espulgas, S. Degradation of chlorophenols by means of advanced oxidation processes: A general review. *Appl. Catal. B: Environ.* **2004**, *47*, 219.
- (22) Hidaka, H.; Ihara, K.; Fujita, Y.; Yamada, S.; Pelizzetti, E.; Serpone, N. Photodegradation of surfactants IV: Photodegradation of non-ionic surfactants in aqueous titanium dioxide suspensions. *J. Photochem. Photobiol. A: Chem.* **1988**, *42*, 375.
- (23) Hidaka, H.; Yamada, S.; Suenaga, S.; Kubota, H.; Serpone, N.; Pelizzetti, E.; Grätzel, M. Photodegradation of surfactants V. Photocatalytic degradation of surfactants in the presence of semiconductor particles by solar exposure. *J. Photochem. Photobiol. A: Chem.* **1989**, *47*, 103.
- (24) Hidaka, H.; Yamada, S.; Suenaga, S.; Zhao, J. Photodegradation of surfactants VI. Complete photocatalytic degradation of anionic, cationic and nonionic surfactants in aqueous semiconductor dispersions. *J. Mol. Catal.* **1990**, *59*, 279.
- (25) Hidaka, H.; Zhao, J.; Suenaga, S.; Serpone, N.; Pelizzetti, E. Photodegradation of surfactants VII. Peroxide and aldehyde formation in the photocatalysed oxidation of nonionic surfactants. *J. Jpn. Oil Chem. Soc.* **1990**, *39*, 963.
- (26) Hidaka, H.; Zhao, J.; Kitamura, K.; Nohara, K.; Serpone, N.; Pelizzetti, E. Photodegradation of surfactants IX: The photocatalysed oxidation of polyoxyethylene alkyl ether homologues at TiO<sub>2</sub>–water interfaces. *J. Photochem. Photobiol. A: Chem.* **1992**, *64*, 103.
- (27) Zhao, J.; Hidaka, H.; Takamura, A.; Pelizzetti, E.; Serpone, N. Photodegradation of surfactants. 11.  $\zeta$ -Potential measurements in the photocatalytic oxidation of surfactants in aqueous TiO<sub>2</sub> dispersions. *Langmuir* **1993**, *9*, 1646.
- (28) Sherrard, K. B.; Marriott, P. J.; McCormick, M. J. Electro spray mass spectrometric analysis and photocatalytic degradation of polyethoxylate surfactants used in wool scouring. *Anal. Chem.* **1994**, *66*, 3394.
- (29) Sherrard, K. B.; Marriott, P. J.; Amiet, R. G.; Colton, R.; McCormick, M. J.; Smith, G. C. Photocatalytic degradation of secondary alcohol ethoxylate: Spectroscopic, chromatographic, and mass spectrometric studies. *Environ. Sci. Technol.* **1995**, *29*, 2235.
- (30) Dube, S.; Nageswara Rao, N. Rate parameter independence on the organic reactant: A study of adsorption and photocatalytic oxidation of surfactants using MO<sub>3</sub>-TiO<sub>2</sub> (M  $\equiv$  Mo or W) catalysts. *J. Photochem. Photobiol. A* **1996**, *93*, 71.
- (31) Sherrard, K. B.; Marriott, P. J.; Gary Amiet, R.; McCormick, M. J.; Colton, R.; Millington, K. Spectroscopic analysis of heterogeneous photocatalysis products of nonylphenol- and primary alcohol ethoxylate nonionic surfactants. *Chemosphere* **1996**, *33*, 1921.
- (32) Delanghe, B.; Mekras, C. I.; Graham, N. J. Aqueous ozonation of surfactants: A review. *Ozone Sci. Eng.* **1991**, *13*, 639.
- (33) Narkis, N.; Schneider-Rotel, M. Volatile organic acids in raw wastewater and in physico-chemical treatment. *Water Res.* **1980**, *14*, 1225.
- (34) Calvosa, L.; Monteverdi, A.; Rindone, B.; Riva, G. Ozone oxidation of compounds resistant to biological degradation. *Water Res.* **1991**, *25*, 985.
- (35) Kitis, M.; Adams, C. D.; Daigger, G. T. The effects of Fenton's reagent pretreatment on the biodegradability of nonionic surfactants. *Water Res.* **1999**, *33*, 2561.
- (36) The Dow Chemical Company, Material Safety Data Sheet, 02/24/2003, Product Name: TERGITOL NP-9 Surfactant.
- (37) Charuk, J. H. M.; Grey, A. A.; Reithmeier, R. A. F. Identification of the synthetic surfactant nonylphenol ethoxylate: a P-glycoprotein substrate in human urine. *Am. J. Physiol. Renal Physiol.* **1998**, *274*, 1127.
- (38) Hatchard, C. G.; Parker, C. A. A new sensitive chemical actinometer. II. Potassium ferrioxalate as a standard chemical actinometer. *Proc. R. Soc. London A* **1956**, *235*, 518.
- (39) Ding, X.; Mou, S.; Zhao, S. Analysis of benzyldimethyldocecylammonium bromide in chemical disinfectants by liquid chromatography and capillary electrophoresis. *J. Chromatogr. A* **2004**, *1039*, 209.
- (40) Shao, B.; Hu, J.; Yang, M. Determination of nonylphenol ethoxylates in the aquatic environment by normal phase liquid chromatography-electrospray mass spectrometry. *J. Chromatogr. A* **2002**, *950*, 167.
- (41) Marcomini, A.; Di Corcia, A.; Samperi, R.; Capri, S. Reversed-phase high-performance liquid chromatographic determination of linear alkylbenzene sulphonates, nonylphenol polyethoxylates and their carboxylic biotransformation products. *J. Chromatogr.* **1993**, *644*, 59.
- (42) Nash, T. The colorimetric estimation of formaldehyde by means of the Hantzsch reaction. *Biochem. J.* **1953**, *55*, 416.
- (43) Kratochvilová, K.; Hoskovicová, I.; Jirkovský, J.; Klíma, J.; Ludvík, J. A spectroelectrochemical study of chemisorption, anodic polymerization and degradation of salicylic acid on conductor and TiO<sub>2</sub> surfaces. *Electrochim. Acta* **1995**, *40*, 2603.
- (44) Burrows, H. D.; Canle, M. L.; Santaballa, J. A.; Steenken, S. Reaction pathways and mechanisms of photodegradation of pesticides. *J. Photochem. Photobiol. B: Biol.* **2002**, *67*, 71.
- (45) Pignatello, J. J.; Liu, D.; Huston, P. Evidence for an Additional Oxidant in the Photoassisted Fenton Reaction. *Environ. Sci. Technol.* **1999**, *33*, 1832.
- (46) Safarzadeh-Amiri, A.; Bolton, J. R.; Cater, S. R. The use of iron in advanced oxidation processes. *J. Adv. Oxid. Technol.* **1996**, *1*, 18.
- (47) Pignatello, J. J. Dark and photoassisted Fe<sup>3+</sup>-catalyzed degradation of chlorophenoxy herbicides by hydrogen peroxide. *Environ. Sci. Technol.* **1992**, *26*, 944.

Received for review November 11, 2009

Revised manuscript received December 31, 2009

Accepted January 5, 2010

IE901785J